Geodetic Control of the Madrid DSS65 VLBI Antenna

Dirk Behrend and Antonio Rius

Institut d'Estudis Espacials de Catalunya (IEEC),
Edif. Nexus-204, Gran Capità 2-4, 08034 Barcelona, Spain

1 Introduction

The NASA Madrid Deep Space Communications Complex (MDSCC), Spain, DSS65 VLBI antenna participates in the European geodetic VLBI network for determining horizontal as well as vertical crustal motion in Europe. In order to prevent local (site) movements from diluting the VLBI-derived plate motions the stability of the antenna over time must be secured. This is usually done by monitoring the stability of the reference point of the antenna which can be defined as the intersection point of the azimuth and elevation axes of the antenna.

In this report we investigate the stability of the DSS65 antenna using geodetic surveillance data taken by the Instituto Geográfico Nacional (IGN), Spain, at different epochs. Futhermore, we discuss the possibility of using levelling data of the azimuth runner level in order to determine the location of the reference point by means of an upward continuation model and to infer stability evidence from this.

2 Antenna Stability by a Multiple Intersection Technique

The standard procedure to monitor the stability of an antenna site is to look into geodetic surveillance data. To this end a local geodetic network has been set up at the MDSCC site consisting of 13 stations and having an inter-station separation of some 100 m. The stations are realized through massive concrete pillars and are tied to the higher order regional net. For the determination of the reference point of the DSS65 antenna a subnet of 6 stations was selected (see figure 1). The selection criteria were mainly good visibility of and short distance to the antenna. For the actual observations Wild T2 theodolites were mounted on the pillars of these stations. An additional station (MIRADOR) was chosen in order to have a well-defined reference for direction measurements. Figure 1 gives an overview of the local subnet including the DSS65 antenna. In the further evaluation it is assumed that the coordinates of the reference stations were stable over the past decade, i.e. that they did not show significant changes (> 0.5 mm).

Following the same observation scheme the IGN performed 4 measurement campaigns (December 1988, March 1997, June 1997, and April 1998):

- The VLBI antenna was equipped with two markers (yellow and red) at the two extreme ends of the elevation axis. They have a diameter of about 3 cm and a height of approx. 2 cm.

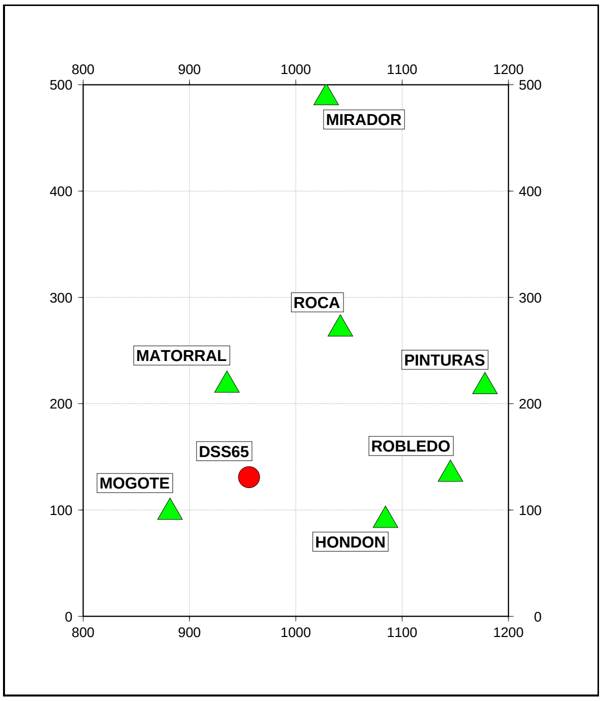

Fig. 1: Local geodetic subnet (6+1 stations) utilized in the geodetic measurements of the DSS65 VLBI antenna. Adding a constant of 393 000 m to the abscissae and 4 476 000 m to the ordinates results in UTM30 coordinates.

- The VLBI antenna was brought into the zenithal position and steered to the azimuth of 0°.
- From the local geodetic network direction and zenith angle measurements were taken to the markers.
- After a complete observation set the antenna was rotated about its azimuth axis and every 30° further sets were taken.

The two campaigns in 1997 are due to a repair work of the azimuth runner level (replacement of tracks and wheels) in April/May 1997 for which the upper part of the antenna was lifted up. This could have affected the location of the reference point creating a discontinuity in the VLBI data. With the help of the two campaigns such a discontinuity can be bridged.

Using all four data sets it is possible to determine 3D-coordinates of the reference point as well as changes thereof over time. The evaluation shall be broken down into the determination of the horizontal position and of the height. The former is used to check the horizontal stability, whereas the latter is taken to control the vertical stability.

2.1 Horizontal Stability

The determination of the horizontal coordinates is equivalent to finding the location of the azimuth axis. As the antenna was rotated about its azimuth axis in the observation procedure the two markers describe two concentric circles with the azimuth axis as the centre location.

2.1.1 Computational Procedure

The computation of the horizontal coordinates (UTM30) for the reference point shall be split as follows:

1. computation of the horizontal coordinates of the markers for the different positions of the VLBI antenna;
2. fitting of two concentric circles to these locations.

These two adjustment problems will be discussed in more detail in the following.

(a) UTM30 coordinates of the two markers

The available observables for computing UTM30 coordinates of the two markers in the different antenna positions are the direction observations taken from the 6 stations of the local subnet whose UTM30 coordinates are considered to be known and errorless. The computation of the unknown coordinates is equivalent to a multiple intersection method which can be solved in a least squares adjustment (Gauss-Markov model). The observation equation reads:

$$r_{i,N} = \arctan\left(\frac{x_N - x_i}{y_N - y_i}\right) + o_i \ .$$

In this equation the index i represents an arbitrary known station, whereas N stands for an unknown point. The unknown parameters are the coordinates of $N(x, y)$ (i.e. of a marker position) and the orientation unknown o_i of the direction observations on the known station. $r_{i,N}$ is the direction observation itself.

After linearization of the observation equation $\underline{\mathrm{L}} = \boldsymbol{\psi}(\underline{\mathrm{X}})$ with a Taylor expansion and introduction of approximate values for the parameters $\underline{\mathrm{X}}_{\mathbf{0}}$ a solution to the adjustment problem is found by

$$\underline{\hat{\mathrm{X}}} = \underline{\mathrm{X}}_{\mathbf{0}} + (\underline{\mathrm{A}}^{\mathrm{T}} \cdot \underline{\mathrm{P}} \cdot \underline{\mathrm{A}})^{-1} \, \underline{\mathrm{A}}^{\mathrm{T}} \cdot \underline{\mathrm{P}} \cdot \underline{\boldsymbol{\ell}} \, ,$$

where the design matrix and the reduced observation vector are

$$\underline{\mathrm{A}} = \left(\frac{\partial \boldsymbol{\psi}(\underline{\mathrm{X}})}{\partial \underline{\mathrm{X}}}\right)_0 \, ,$$

$$\underline{\boldsymbol{\ell}} = \underline{\mathrm{L}} - \boldsymbol{\psi}(\underline{\mathrm{X}}_{\mathbf{0}}) \ .$$

The weight matrix is defined as the inverse of the co-factor matrix of the observations which, according to the stochastical model, is the covariance matrix of the observations divided by the variance of the unit weight (a priori):

$$\underline{\mathrm{P}} = \underline{\mathrm{Q}}_{\ell\ell}^{-1} = \left(\frac{1}{\sigma_0^2} \, \boldsymbol{\Sigma}_{\ell\ell}\right)^{-1} \ .$$

In the problem at hand there are 48 (= 2 markers $\cdot$ 2 coordinates $\cdot$ 12 points) coordinate parameters (if all marker positions are to be determined) and 6 orientation parameters to be solved for. Hence, an adjustment problem is given if at least 55 direction measurements are taken. As the observations are considered to be uncorrelated and of the same accuracy, the weight matrix becomes the identity matrix: $\underline{\mathrm{P}} = \underline{\mathrm{I}}$.

(b) Fitting of two concentric circles

The UTM30 coordinates of the marker positions (red and yellow) are used as input for the following least squares fitting of two concentric circles. In this case the unknowns are the UTM30 coordinates of the centre (x_c, y_c) of the two circles as well as the two radii R_a. The functional model can be formulated as follows:

$$\boldsymbol{\psi}(\underline{\mathrm{L}}, \underline{\mathrm{X}}) = (x_{i_a} - x_c)^2 + (y_{i_a} - y_c)^2 - R_a^2 = 0 \;,$$

where the subscript a represents the red and the yellow marker, resp. A Taylor expansion (limited to first order terms) yields the linearized functional model

$$\underset{r,n}{\underline{\mathrm{B}}} \cdot \underset{n,1}{\underline{\mathrm{v}}} + \underset{r,n}{\underline{\mathrm{A}}} \cdot \underset{u,1}{\hat{\underline{\boldsymbol{x}}}} + \underset{r,1}{\underline{\mathrm{w}}} = \underset{r,1}{\underline{0}}$$

with the design matrices

$$\underset{r,u}{\underline{\mathrm{A}}} = \frac{\partial \boldsymbol{\psi}(\underline{\mathrm{L}}, \underline{\mathrm{X}})}{\partial \underline{\mathrm{X}}} \;,$$

$$\underset{r,n}{\underline{\mathrm{B}}} = \frac{\partial \boldsymbol{\psi}(\underline{\mathrm{L}}, \underline{\mathrm{X}})}{\partial \underline{\mathrm{L}}} \;,$$

and the misclosure vector

$$\underset{r,1}{\underline{\mathrm{w}}} = \boldsymbol{\psi}(\underline{\mathrm{L}}, \underline{\mathrm{X}}_{\mathbf{0}})$$

where n denotes the number of observations, r the number of conditions, and u the number of unknowns.

The stochastical model shall be

$$\underline{\boldsymbol{\Sigma}}_{\boldsymbol{\ell\ell}} = \sigma_0^2 \, \underline{\mathrm{Q}}_{\boldsymbol{\ell\ell}}$$

where the covariance matrix $\underline{\boldsymbol{\Sigma}}_{\boldsymbol{\ell\ell}}$ of the observations equals the covariance matrix of the marker positions determined in the previous adjustment.

A solution of the adjustment problem at hand is obtained by introducing the condition that the sum of the weighted residuals shall be a minimum. This condition plus the linearized functional model lead to a Lagrangian extreme value problem which, in turn, leads to the formation of the normal equations:

$$\begin{bmatrix} \underset{r,n}{\underline{\mathrm{B}}} \cdot \underset{n,n}{\underline{\mathrm{Q}}_{\boldsymbol{\ell\ell}}} \cdot \underset{n,r}{\underline{\mathrm{B}}}^{\mathrm{T}} & \underset{r,u}{\underline{\mathrm{A}}} \\ \underset{u,r}{\underline{\mathrm{A}}}^{\mathrm{T}} & \underset{u,u}{\underline{0}} \end{bmatrix} \begin{bmatrix} \underset{r,1}{\underline{\mathrm{k}}} \\ \underset{u,1}{\underline{0}} \end{bmatrix} + \begin{bmatrix} \underset{r,1}{\underline{\mathrm{w}}} \\ \underset{u,1}{\underline{0}} \end{bmatrix} = \underset{r+u,1}{\underline{0}} \;.$$

The normal equations are solved by inverting the normal matrix:

$$\begin{bmatrix} \underset{r,r}{\underline{\mathrm{Q}}_{\mathbf{11}}} & \underset{r,u}{\underline{\mathrm{Q}}_{\mathbf{12}}} \\ \underset{u,r}{\underline{\mathrm{Q}}_{\mathbf{21}}} & \underset{u,u}{\underline{\mathrm{Q}}_{\mathbf{22}}} \end{bmatrix} = \begin{bmatrix} \underset{r,n}{\underline{\mathrm{B}}} \cdot \underset{n,n}{\underline{\mathrm{Q}}_{\boldsymbol{\ell\ell}}} \cdot \underset{n,r}{\underline{\mathrm{B}}}^{\mathrm{T}} & \underset{r,u}{\underline{\mathrm{A}}} \\ \underset{u,r}{\underline{\mathrm{A}}}^{\mathrm{T}} & \underset{u,u}{\underline{0}} \end{bmatrix}^{-1} \;.$$

The adjusted parameters (position of circle centre, radii) are given by

$$\hat{\underline{\mathrm{X}}} = \underline{\mathrm{X}}_{\mathbf{0}} - \underline{\mathrm{Q}}_{\mathbf{21}} \cdot \underline{\mathrm{w}} \;.$$

Their accuracy can be taken from the covariance matrix of the parameters

$$\underline{\boldsymbol{\Sigma}}_{\boldsymbol{xx}} = s_0^2 \, \underline{\mathrm{Q}}_{\boldsymbol{xx}} = - \, s_0^2 \, \underline{\mathrm{Q}}_{\mathbf{22}}$$

with the empirical variance of the unit weight

$$s_0^2 = \frac{\left(\underline{\mathbf{Q}}_{\mathbf{11}}\ \underline{\mathrm{w}}\right)^{\mathrm{T}}\ (\underline{\mathrm{w}} + \underline{\mathrm{A}}\ \hat{\underline{\mathrm{x}}})}{r - u}$$

and $f = r - u$ the degrees of freedom. Here the empirical value s_0^2 is favoured before the theoretical one (σ_0^2), as s_0^2 reflects the actual conditions prevailing during the time of observation. The theoretical value may be used in simulation studies.

2.1.2 Numerical Results

Using this evaluation procedure all four campaigns have been analysed. After several tests the a priori standard deviation of the direction observations was chosen to $s_r = \pm 1.2$ mgon. The adjustment of the horizontal net resulted in coordinates for the single marker positions with standard deviations of $\pm 1 \ldots 8$ mm. These points were fitted to two concentric circles resulting in UTM30 coordinates for the reference point at the different epochs (cf. table 1).

Tab. 1: Horizontal position (UTM30 coordinates) of the DSS65 reference point determined at different epochs.

Campaign	**Northing** [m]	**Easting** [m]	**s.d. (N)** [mm]	**s.d. (E)** [mm]
December 88	4 476 130.9987	393 955.9346	±1.2	±1.2
March 97	131.0053	955.9328	±2.5	±2.6
June 97	130.9983	955.9343	±2.8	±2.9
April 98	130.9984	955.9338	±1.3	±1.3

The standard deviations (1σ) of the UTM30 coordinates of the reference point are in the range of $\pm 1 \ldots 3$ mm. Accordingly, the DSS65 antenna can be considered stable (i.e. showing no significant change) over the time span of 10 years at least in the east component. In the north component there was a change of 7 mm which only showed up in March 97. The physical meaning and/or the exclusion of errors (e.g. human error, modelling error) are still under investigation.

2.2 Vertical Stability

The determination of the height of the reference point (orthometric heights referring to the tide gauge at Alicante) follows a relatively simple procedure. As there were no distance measurements taken the necessary distance information is to be taken from the horizontal adjustment resp. the computed horizontal coordinates (cf. section 2.1).

2.2.1 Computational Procedure

The height transfer from the pillars to the single marker positions had to be done by trigonometric levelling. Thus, the control of the vertical stability was also split into two steps:

1. trigonometric height determination (distance taken from horizontal adjustment) for the different marker positions;

2. computation of weighted means $\overline{H}$ for the two markers and a simple mean thereof:

$$\overline{H} = \frac{g_1 H_1 + \ldots + g_n H_n}{g_1 + \ldots + g_n}$$

$$s_{\overline{H}}^2 = \frac{s^2}{g_1 + \ldots + g_n}$$

The weights g_i are the quotients of an arbitrary unit variance s^2 and the variance of the single height determinations:

$$g_i = \frac{s^2}{s_i^2}$$

Here the largest variance of the single determinations is taken as the unit variance.

The two weighted means (red and yellow) are averaged (simple mean) to give a height which corresponds more or less to the height of the reference point. There probably exists a small difference to the true value as the two markers might not be exactly mounted in prolongation of the elevation axis. Hence, the obtained height of the reference point is biased by an unknown value. Since most of the users are solely interested in height changes and not in the height itself, these heights are still of value. Also the weighted means for the red and yellow marker can be utilized for monitoring height changes.

2.2.2 Numerical Results

Following the procedure outlined in section 2.2.1 first heights of the single marker positions have been determined. The height values vary during a full completion of a circle between 6 mm (December 88) and 16 mm (March 97). The standard deviations are in the range of $\pm 2 \ldots 6$ mm. Then weighted means for the two markers separately and a simple average thereof was computed (cf. table 2).

Tab. 2: Weighted means for the heights of the two markers and simple average thereof for all campaigns.

Campaign	**Height of Marker** red [m]	yellow [m]	**s.d. (r)** [mm]	**s.d. (y)** [mm]	**Simple Mean** [m]
December 88	781.2537	781.2612	±0.9	±0.6	781.257
March 97	781.2682	781.2784	±1.6	±1.1	781.273
June 97	781.2766	781.2844	±1.8	±1.1	781.281
April 98	781.2726	781.2837	±1.8	±1.1	781.278

The standard deviations of the weighted means are in the range of $\pm 1 \ldots 2$ mm. Hence, there are two significant height changes in the past decade: an uplift of about 17 mm in the time from 1988 to 1997 and a further rise of 6 mm from March 97 to June 97. The latter can be attributed to the runner level repair performed in between the campaigns. In the time from June 97 to April 98 the antenna eventually stabilized, i.e. only an insignificant change of -0.7 mm has been found.

3 Antenna Stability using Runner Level Data

In section 2 the antenna stability was checked with the help of four geodetic measurement campaigns. Unfortunately, there is a large time span between the first and the second epoch of almost 9 years. Hence, the utilization of other data sets for the stability control should be considered and investigated in order to be able to fill this time gap.

As part of the station monitoring program the azimuth runner level is spirit levelled (accuracy of ± 0.2 mm) relative to the real azimuth of 200°. The measurements are done on a monthly basis and have been taken for the first time in 1991. For the intended investigation the levelling results from March 97 have been chosen, because then the data showed the largest height variation in the runner level of up to 17 mm (cf. figure 2) and, furthermore, an IGN campaign is available for the same period.

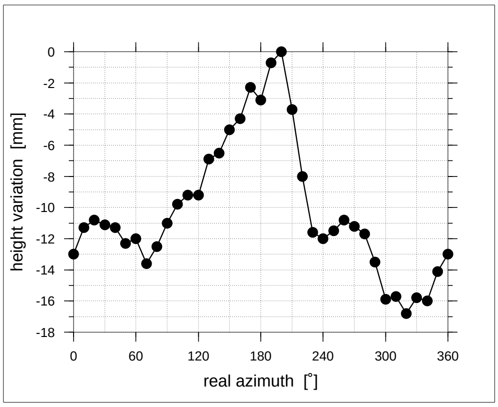

Fig. 2: Height variations of the azimuth runner level w.r.t. the real azimuth of 200° (March 97).

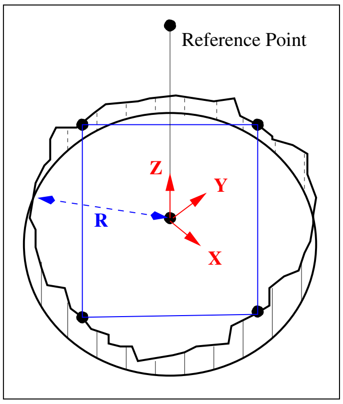

Fig. 3: Simple rigid body model used in the upward continuation process.

The upper part of the antenna moves on 4 wheels on the azimuth runner level. In a least squares sense these wheels define a plane which alters its parameters according to the location of the wheels on the runner level (figure 3). Assuming that the whole antenna follows the tilting of this plane (simple rigid body model), 3D-displacements of the reference point can be determined, i.e. height variations of the runner level are modelled into variations of the reference point.

The upward continued height variations induce displacements of the “reference point” with variations of 4 . . . 6 mm where the “mountain” in the runner level shows up as 4 peaks (figure 4). The error estimates have at least the same size as the signal. Hence, it appears that the simple tilted rigid body model is insufficient for upward continuing the runner level variations. This is supported by the fact that the model displacements do not correlate with the results from the IGN data, i.e. the computed Pearson correlation coefficients are close to zero. Hopefully, a refinement of the upward continuation model will cure this deficiency.

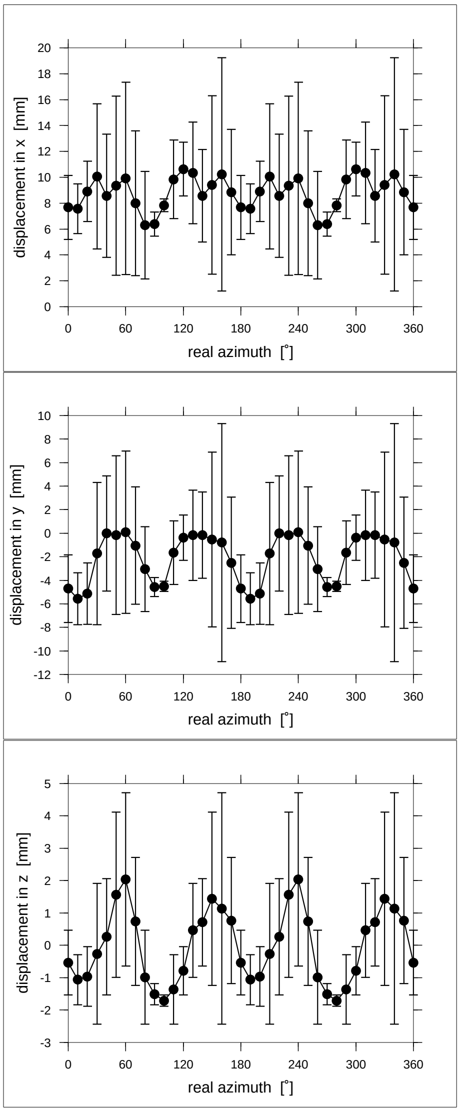

Fig. 4: Displacements (including error bars) of the reference point caused by variations in the azimuth runner level (simple tilted rigid body model).

4 Conclusions

In this study geodetic surveillance data have been analysed to control the stability of the DSS65 VLBI antenna. A least squares evaluation procedure yielded 3D-coordinates of the antenna reference point with an accuracy of a few mm. Thus, the antenna can be considered stable in position (showing no significant change) over the past decade. This excludes a significant 7 mm change in the north component in March 97. The height, on the other hand, has undergone two significant height changes: an uplift of 17 mm from December 88 to March 97 and an uplift of 6 mm from March 97 to June 97. The latter can be attributed to the azimuth runner level repair in April/May 97. In the time from June 97 to April 98 the antenna eventually stabilized. A new observation campaign is planned for this spring/summer.

In order to fill a time gap of about 9 years in the geodetic surveillance data a simple model for propagating height variations of the azimuth runner level to the reference point has been developed. This model proved the general possibility of an upward continuation, but also revealed its limitations.

Acknowledgements. This research work was supported by the European Union under the TMR network grant FMRX-CT960071 “Measurement of Vertical Crustal Motion in Europe by VLBI”. We are grateful to the geodetic division of the Instituto Geográfico Nacional (Antonio Barbadillo) for providing the original data of the field campaigns. Furthermore, the provision of the levelling data of the azimuth runner level by the MDSCC (Jose Urech) is gratefully acknowledged.